

## Rock Slope Stability Assessment of Limestone Hills in Northern Kinta Valley, Ipoh, Perak, Malaysia

GOH THIAN LAI<sup>1\*</sup>, AINUL MARDHIYAH MOHD RAZIB<sup>1</sup>, NUR AMANINA MAZLAN<sup>1</sup>, ABDUL GHANI RAFEK<sup>2</sup>, AILIE SOFYIANA SERASA<sup>3</sup>, NORBERT SIMON<sup>1</sup>, NORAINI SURIP<sup>3</sup>, LEE KHAI ERN<sup>4</sup> AND TUAN RUSLI MOHAMED<sup>5</sup>

<sup>1</sup>School of Environmental and Natural Resource Sciences, Faculty of Science and Technology, Universiti Kebangsaan Malaysia, 43600 UKM Bangi, Selangor Darul Ehsan, Malaysia

<sup>2</sup>Department of Geosciences, Universiti Teknologi PETRONAS, Bandar Seri Iskandar, 31750 Tronoh, Perak Darul Ridzuan, Malaysia

<sup>3</sup>Chemical and Petroleum Engineering Department, Faculty of Engineering, Technology and Built Environment, UCSI University, 56000 Cheras, Malaysia

<sup>4</sup>Institute for Environment and Development (LESTARI), Universiti Kebangsaan Malaysia, 43600 UKM Bangi, Selangor, Malaysia.

<sup>5</sup>Department of Mineral and Geoscience Malaysia Perak, Jalan Sultan Azlan Shah, 31400 Ipoh, Perak, Malaysia

\*Corresponding author: [gdsbgoh@gmail.com](mailto:gdsbgoh@gmail.com)

This is an open access article distributed under the Creative Commons Attribution License, which permits unrestricted use, distribution, and reproduction in any medium, provided the original work is properly cited

### ARTICLE DETAILS

### ABSTRACT

#### Article history:

Received 27 September 2016

Accepted 13 December 2016

Available online 10 January 2017

#### Keywords:

Limestone, failure modes, rock slope stability assessment

The uniqueness of karst topography in Kinta Valley lies with the spectacular shape of the steep-sided limestone towers. However, the instability of these hillslopes may affect the vulnerability of the surrounding area. Thus, this study was conducted with the objective to investigate the failure modes of 9 slopes in the vicinity of northern Kinta Valley, Ipoh, Perak. There were two types of failure modes identified in the study area, which are planar and wedge failures. Planar failures were identified on slope GL3 of Gunung Lang and slope GR3 of Gunung Rapat with the dip direction and dip angle of 280°/79° and 004°/64° respectively. Two wedge failures were identified on slope QXL1 of Qing Xing Ling, Taman Saikat with dip direction and dip angle of 252°/82° and 302°/74° respectively. A wedge failure was identified on slope GL3 for Gunung Lang, slope GR1, slope GR3 for Gunung Rapat and slope QXL2 for Qing Xing Ling, Taman Saikat. The dip direction and dip angle for the respective wedges failure were 345°/65°, 036°/49°, 006°/64° and 025°/60°. No failure was identified on slope GL1, and slope GL2, for Gunung Lang and slope GR2, and slope GR4 for Gunung Rapat.

## 1. INTRODUCTION

Karst topography in Kinta Valley is characterised by the steep-sided limestone hills and decorated with many limestone morphological features such as caves and dolines. Kinta Valley has been proposed to be developed as one of the national geoparks in Malaysia due to its impressive beautiful landscape (Leman, 2013). A literature study revealed that less research studies have been conducted on limestone hills' rock slope stability assessment. The local researchers were focused more on rock mass classification (Norbert et al. 2016), landslide (Norbert et al. 2013, Norbert et al. 2014, Norbert et al. 2015a), rock fall (Norbert et al. 2015b) and prediction of uniaxial compressive strength using ultrasonic (Goh et al. 2016, Goh et al. 2015a, Goh et al. 2015b, Goh et al. 2014b). Ghani Rafek et al. (2012), Ghani et al. (2011) and Goh et al. (2012a, 2014a) characterized the roughness of discontinuities surface by established a polynomial relationship between JRC with peak friction angles schist and granite. Goh et al. (2012b) investigated the influence of conditions of weathering to the Geomechanical strength of Granites and Schists. Abdul Ghani Rafek et al. (2015) assessed the Kinta limestone based on slope mass rating. Geohazard incidents like rock slab detachment and rock falls might occur as a result of weathering processes and discontinuity factors characterised mainly by geological structure conditions such as jointing, fractures and daylighting of discontinuities. These geological hazards will affect the vulnerability of development in the encompassing areas (Shu & Lai, 1974). The impact of a rockfall can also affect its surrounding in which the air blast resulting from the fallen rock debris can be felt at a distance that is much further from the catastrophe area which could affect nearby buildings (Lai, 1974, Shu & Lai, 1974).

As stated by Shu and Lai (1973), reports on the instability of limestone hills such as at Gunung Cheroh in the Kinta Valley have been a subject of investigations by the Geological Survey of Malaysia in early 1927. One of the incidents of rockfall tragedy had occurred at Gunung Cheroh, Ipoh, Perak which caused the demise of 40 people in October, 1973 (Shu & Lai 1974). Rock fall incident at Gunung Pondok, Perak were also reported by Shu and Razak (1984).

Structural failure has been reported as the main causal factor of the rockfall events. Chemical weathering process also contributes to the decomposition of the rock mass. According to Chow and Sahat (1988) chemical weathering from water dissolution and quarry activities were reported to be the main causal factors of rockfalls such as the incident which occurred at Gunung

Tunggal. It was reported that the cohesive strength along joints and fractures had decreased due to chemical weathering which possibly caused the rockfall.

With regard to these issues, this research was conducted to investigate the failure modes of eight limestone hills in the Kinta Valley by using kinematic analysis as recommended by Hoek and Bray (1981). The examples of rockfall events in the Kinta Valley that had caused a number of fatality and damages to vehicles and civil structures are shown in Table 1.

Table 1: Examples of rockfall occurrences in the Kinta Valley that had caused a number of deaths and damages to vehicles and civil structures

| Location  | Date             | Damage/fatalities  |
|---|------------------|--|
| East of Gunung Cheroh, Ipoh                         | 18 October 1973  | A long house was destroyed by rock debris and caused 40 deaths |
| West of Gunung Rapat, Kg. Sengat                    | 21 October 1976  | Damage to vehicles but no fatalities                           |
| Northeast of Gunung Karang Besar, Keramat Pulai     | Before 1981      | No damage to structure or fatalities reported                  |
| Northwest of the Gunung Karang Besar, Keramat Pulai | Before 1981      | No damage to structure or fatalities reported                  |
| West of Gunung Karang Kecil, Keramat Pulai          | Before 1981      | No damage to structure or fatalities reported                  |
| East of Gunung Tunggal, Gopeng                      | 29 December 1987 | Damage to structure (an office) and 1 fatality                 |
| North of Gunung Lang                                | Before 1993      | No damage to structure or fatalities reported                  |
| Gunung Karang Besar, Keramat Pulai                  | 5 June 2008      | Damage to vehicle and 1 death                                  |
| Yee Lee Edible Oils Factory                         | 13 February 2012 | Damage to structure but no fatalities reported                 |
| Gunung Lang, Ipoh                                   | 13 February 2012 | Damage to structure but no fatalities reported                 |
| Gua Tempurung, Kampar                               | 11 April 2012    | No damage to structure or fatalities reported                  |

Source: Simon et al. (2015)

## MATERIALS AND METHODOLOGY

### Geology of Study Areas

The study area is located in the Kinta Valley, Perak as shown in Figure 1. The study areas covered the massive limestone bodies that are heavily jointed and fractured. As stated by Simon et al. (2015), there are numerous massive limestone hills with an average size of 1.08

km<sup>2</sup> with maximum elevation of these hills reaching 546 m based on the topographic map. The localized, highly weathered schist was found at the bottom of a massive limestone body which can be observed in a cave located at Gunung Rapat. This limestone bodies were named by Foo (1983) as Kinta Limestone Formation with age of Silurian to Permian.

**Methodology**

Discontinuity surveys were conducted by using the scan line method as suggested by Priest and Hudson (1976) and ISRM (1978) where 10 discontinuity parameters were considered. The parameters are dip direction, dip angle, discontinuity length (persistence), aperture, surface roughness, infilling, weathering, groundwater conditions, number of joint sets and block size.

The kinematic analysis was conducted by using Stereo32 software (Ruhr University Bochum, 2016). The results were interpreted to identify types of failure mode based on Hoek and Bray (1981). According to them, the possible major types of block failures on slopes and structural geology conditions are plane failure, wedge failure, toppling failure and circular failure. The joint roughness coefficient values were used for the determination of peak friction angle as recommended by Ghani Rafek et al. (2012).

**RESULTS AND DISCUSSION**

A total of 9 slopes at the Northern Kinta Valley were assessed and labeled as GL1, GL2, and GL3 for Gunung Lang, GR1, GR2, GR3 and GR4 for Gunung Rapat and QXL1 and QXL2 for Qing Xing Ling, Taman Saikat as shown in Figure 3, Figure 4, Figure 5, Figure 6, Figure 7, Figure 8, Figure 9, Figure 10 and Figure 11, respectively. The locations of respective slopes are shown in Figure 2. The stereographs of respective slope were shown in Figure 12, Figure 13, Figure 14, Figure 15, Figure 16, Figure 17, Figure 18, Figure 19 and Figure 20, respectively. GL1, GL2, and GL3 of Gunung Lang are composed of 5 major joint sets. GR1, GR2, GR3 and GR4 for Gunung Rapat were composed of 4 major joint sets. 4 major joint sets were identified on slope QXL1 and QXL2 for Qing Xing Ling, Taman Saikat. The orientation of major joint sets and slope face of the respective slope are shown in Table 2.

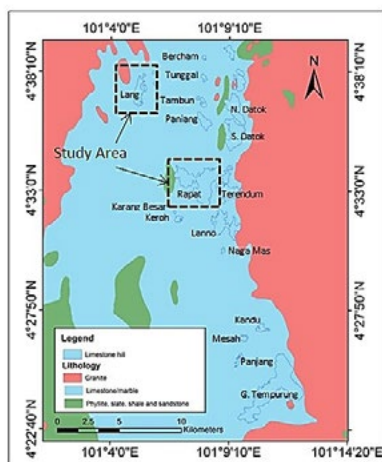


Figure 1: Geological map of Kinta Valley, Ipoh, Perak, Malaysia.

Source: Modified from Norbert *et al.* (2015b)

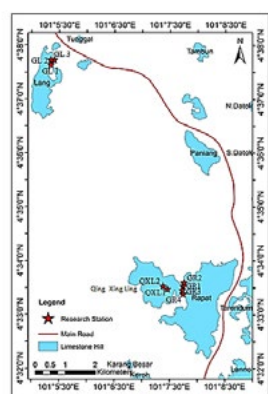


Figure 2: Location map for 9 slopes of study areas in the Northern Kinta Valley, Ipoh, Perak, Malaysia



Figure 3: Slope GL1, Gunung Lang, Ipoh, Perak, Malaysia.



Figure 4: Slope GL2, Gunung Lang, Ipoh, Perak, Malaysia.



Figure 5: Slope GL3, Gunung Lang, Ipoh, Perak, Malaysia.



Figure 6: Slope GR1, Gunung Rapat, Ipoh, Perak, Malaysia.



Figure 7: Slope GR2, Gunung Rapat, Ipoh, Perak, Malaysia.



Figure 8: Slope GR3, Gunung Rapat, Ipoh, Perak, Malaysia.



Figure 9: Slope GR4, Gunung Rapat, Ipoh, Perak, Malaysia.



Figure 10: Slope QXL1, Qing Xing Ling, Taman Saikat, Ipoh, Perak, Malaysia.



Figure 11: Slope QXL2, Qing Xing Ling, Taman Saikat, Ipoh, Perak, Malaysia.

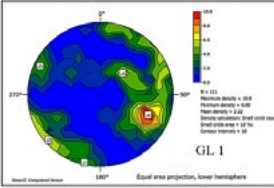


Figure 12: Stereograph for slope GL1, Gunung Lang, Ipoh, Perak, Malaysia.

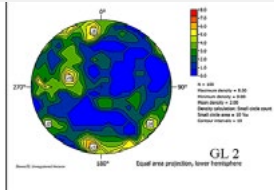


Figure 13: Stereograph for slope GL2, Gunung Lang, Ipoh, Perak, Malaysia.

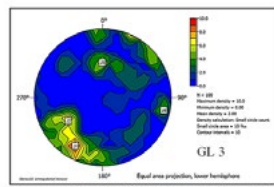


Figure 14: Stereograph for slope GL3, Gunung Lang, Ipoh, Perak, Malaysia.

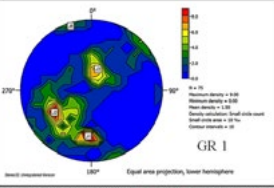


Figure 15: Stereograph for slope GR1, Gunung Rapat, Ipoh, Perak, Malaysia.

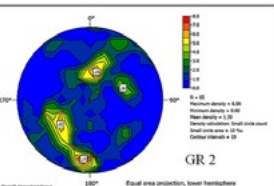


Figure 16: Stereograph for slope GR2, Gunung Rapat, Ipoh, Perak, Malaysia.

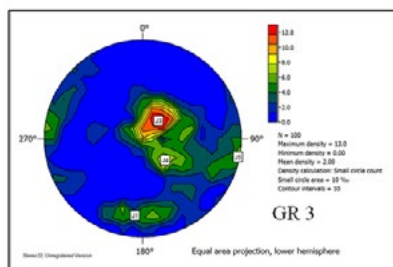


Figure 17: Stereograph for slope GR3, Gunung Rapat, Ipoh, Perak, Malaysia.

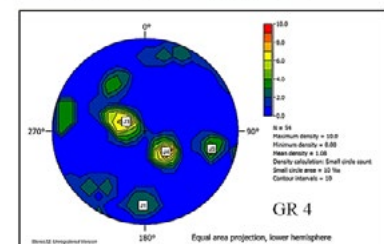


Figure 18: Stereograph for slope GR4, Gunung Rapat, Ipoh, Perak, Malaysia.

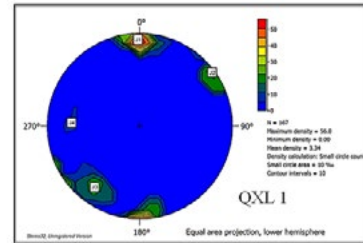


Figure 19: Stereograph for slope QXL1, Qing Xing Ling, Taman Saikat, Ipoh, Perak, Malaysia.

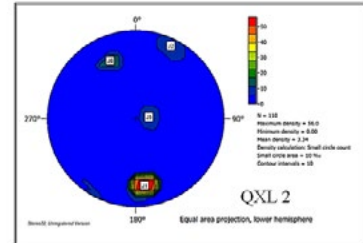


Figure 20: Stereograph for slope QXL2, Qing Xing Ling, Taman Saikat, Ipoh, Perak, Malaysia.

Table 2: Orientation of major joint set and slope face for slopes GL1, GL2 and GL3, for Gunung Lang, Ipoh; GR1, GR2, GR3 and GR4, for Gunung Rapat, Ipoh; QXL1 and QXL2, for Qing Xing Ling, Taman Saikat, Ipoh, Perak, Malaysia.

| Slope | Major Joint set/Slope Face | Dip Direction (°) | Dip Angle (°) |
|-------|----------------------------|-------------------|---------------|
| GL1   | <b>Slope face (SF)</b>     | <b>148</b>        | <b>82</b>     |
|       | J1                         | 013               | 84            |
|       | J2                         | 050               | 83            |
|       | J3                         | 115               | 81            |
|       | J4                         | 293               | 59            |
|       | J5                         | 229               | 36            |
| GL2   | <b>Slope face (SF)</b>     | <b>052</b>        | <b>78</b>     |
|       | J1                         | 007               | 80            |
|       | J2                         | 055               | 84            |
|       | J3                         | 106               | 59            |
|       | J4                         | 309               | 77            |
|       | J5                         | 174               | 70            |
| GL3   | <b>Slope face (SF)</b>     | <b>270</b>        | <b>82</b>     |
|       | J1                         | 030               | 71            |
|       | J2                         | 054               | 51            |
|       | J3                         | 179               | 42            |
|       | J4                         | 280               | 79            |
|       | J5                         | 316               | 82            |
| GR1   | <b>Slope face (SF)</b>     | <b>003</b>        | <b>55</b>     |
|       | J1                         | 060               | 51            |
|       | J2                         | 196               | 25            |
|       | J3                         | 162               | 88            |
|       | J4                         | 262               | 82            |
|       | J5                         | 007               | 77            |
| GR2   | <b>Slope face (SF)</b>     | <b>052</b>        | <b>43</b>     |
|       | J1                         | 193               | 33            |
|       | J2                         | 250               | 40            |
|       | J3                         |                   |               |
|       | J4                         |                   |               |
|       | J5                         |                   |               |
| GR3   | <b>Slope face (SF)</b>     | <b>087</b>        | <b>88</b>     |
|       | J1                         | 004               | 64            |
|       | J2                         | 220               | 19            |
|       | J3                         | 315               | 25            |
|       | J4                         | 280               | 88            |
|       | J5                         | 120               | 84            |
| GR4   | <b>Slope face (SF)</b>     | <b>120</b>        | <b>84</b>     |
|       | J1                         | 001               | 66            |
|       | J2                         | 115               | 18            |
|       | J3                         | 313               | 25            |
|       | J4                         | 285               | 63            |
|       | J5                         | 279               | 83            |
| QXL1  | <b>Slope face (SF)</b>     | <b>279</b>        | <b>83</b>     |
|       | J1                         | 360               | 82            |
|       | J2                         | 238               | 83            |
|       | J3                         | 040               | 60            |
|       | Major joint set (J)        | 093               | 64            |
|       | Slope face (SF)            | 040               | 82            |
| QXL2  | <b>Slope face (SF)</b>     | <b>040</b>        | <b>82</b>     |
|       | J1                         | 354               | 64            |
|       | J2                         | 207               | 79            |
|       | J3                         | 271               | 14            |
|       | J4                         | 157               | 60            |
|       | J5                         |                   |               |

The peak friction angles for respective slopes used in kinematic analysis were determined based on the tilt test method suggested by Abdul Ghani Rafek and Goh (2012). The peak friction angle for slope GL1, GL2, and GL3 for Gunung Lang was 43°. The peak friction angles for slope GR1, GR2, GR3 and GR4 for Gunung Rapat were 43°, 70°, 33° and 49° respectively. The peak friction angle for slope QXL1 and QXL2 for Qing Xing Ling was 49°.

Figure 21, Figure 22, Figure 23, Figure 24, Figure 25, Figure 26, Figure 27, Figure 28 and Figure 29 shows the results of kinematic analysis for respective slopes. Table 3 shows the summary of kinematic analysis for the respective slopes. Wedge and planar failures were identified on slope GL3 for Gunung Lang. The dip direction/dip angle for respective wedge and planar failures were 345°/65° and 280°/79°. No mode of failure was identified on slope GL1 and GL2 for Gunung Lang.

A wedge failure was identified on slope GR1 with the respective dip direction/ dip angle of 036°/49°. A wedge failure and planar failure was identified on slope GR3 for Gunung Rapat with the respective dip direction/ dip angle of 004°/64° and 006°/64°. No mode of failure was identified on slope GR2 and GR4 for Gunung Rapat. There were two wedge failures identified on slope QXL1 and one wedge failure on slope QXL2 for Qing Xing Ling, Taman Saikat. The respective dip direction/dip angle of wedge failures were 252°/82°, 302°/74° and 025°/60°.

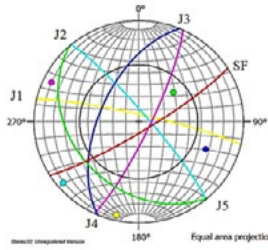


Figure 21: Kinematic analysis for slope GL1, Gunung Lang using friction angle of 43°. No mode of failure on this slope.

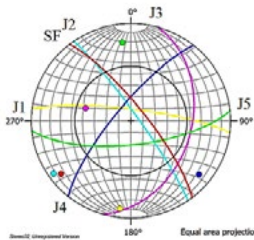


Figure 22: Kinematic analysis for slope GL2, Gunung Lang using friction angle of 43°. No mode of failure on this slope.

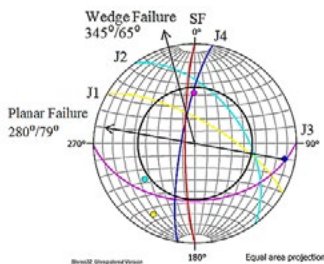


Figure 23: Kinematic analysis for slope GL3, Gunung Lang using friction angle of 43°. From the kinematic analysis, a planar and a wedge failure were identified. The dip direction/dip angle for respective wedge and planar failure were 345°/65° and 280°/79°.

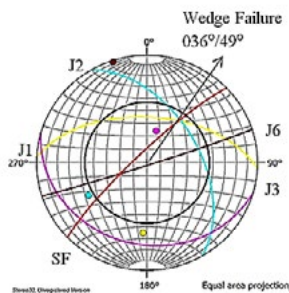


Figure 24: Kinematic analysis for slope GR1, Gunung Rapat using friction angle of 43°. From the kinematic analysis, a wedge failure was identified. The dip direction/dip angle for the wedge failure was 036°/49°.

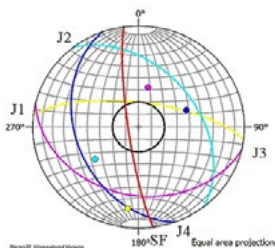


Figure 25: Kinematic analysis for slope GR2, Gunung Rapat using friction angle of 70°. No mode of failure on this slope.

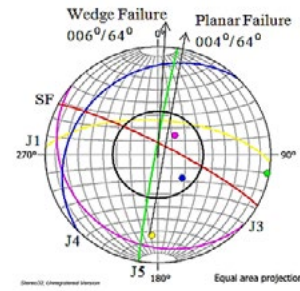


Figure 26: Kinematic analysis for slope GR3, Gunung Rapat using friction angle of 33°. From the kinematic analysis, a planar and a wedge failure were identified. The dip direction/dip angle for respective wedge and planar failure were 006°/64° and 004°/64°.

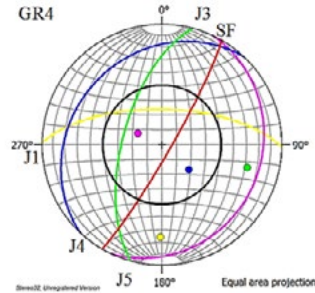


Figure 27: Kinematic analysis for slope GR4, Gunung Rapat using friction angle of 49°. No mode of failure on this slope.

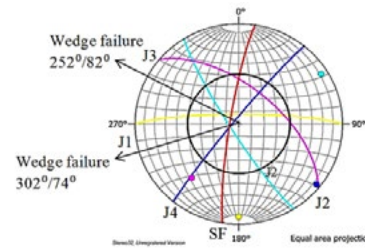


Figure 28: Kinematic analysis for slope QXL1, Qing Xing Ling using friction angle of 49°. From the kinematic analysis, two wedge failures were identified. The dip direction/dip angle for the respective wedge failures were 252°/82° and 302°/74°.

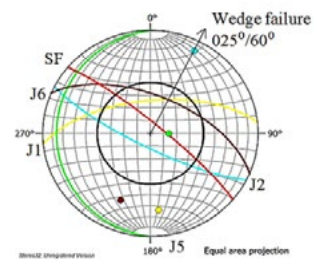


Figure 28: Kinematic analysis for slope QXL2, Qing Xing Ling using friction angle of 49°. From the kinematic analysis, a wedge failure was identified. The dip direction/dip angle for the wedge failure was 025°/60°.

Table 3: Summary of kinematic analysis for slopes GL1, GL2 and GL3, for Gunung Lang, Ipoh; GR1, GR2, GR3, GR4 and GR5, for Gunung Rapat, Ipoh; QXL1 and QXL2, for Qing Xing Ling, Gunung Rapat, Ipoh.

| Slope | Friction angle $\phi$ | Joint Roughness Coefficient (JRC) | Failure Mode  |
|-------|-----------------------|-----------------------------------|---|
| GL1   | 43                    | 5                                 | No failure  |
| GL2   | 43                    | 5                                 | No failure  |
| GL3   | 43                    | 5                                 | Wedge failure: 345°/65°<br>Planar failure: 280°/79° |
| GR1   | 43                    | 5                                 | Wedge failure: 036°/49°                             |
| GR2   | 70                    | 15                                | No failure  |
| GR3   | 33                    | 9                                 | Wedge failure: 006°/64°<br>Planar failure: 004°/64° |
| GR4   | 49                    | 7                                 | No failure  |
| QXL1  | 49                    | 7                                 | Wedge failure: 252°/82°<br>Wedge failure: 302°/74°  |
| QXL2  | 49                    | 7                                 | Wedge failure: 025°/60°                             |

## CONCLUSION

From the kinematic analysis assessment, a wedge failure was identified at on slope GL3, for Gunung Lang. The dip direction and dip angle of the wedge failure was  $345^{\circ}/65^{\circ}$ . There are no modes of failure on slope GL1 and GL2 for Gunung Lang. A wedge failure was identified on slope GR1 for Gunung Rapat with the dip direction and dip angle of  $036^{\circ}/49^{\circ}$ . No modes of failure were identified on slope GR2 for Gunung Rapat. A wedge and planar failure were identified on slope GR3 for Gunung Rapat. The dip direction and dip angle for the respective wedge and planar failure were  $006^{\circ}/64^{\circ}$  and  $004^{\circ}/64^{\circ}$ . No modes of failure were identified on slope GR4 for Gunung Rapat. Two wedge failures were identified on slope QXL1 for Qing Xing Ling, while a wedge failure was identified on slope QXL2 for Qing Xing Ling. The dip direction and dip angle for the respective wedge failures were  $252^{\circ}/82^{\circ}$ ,  $302^{\circ}/74^{\circ}$  and  $025^{\circ}/60^{\circ}$ .

## Acknowledgement

This publication is based on work supported by the Government of Malaysia under grant Fundamental Research Grant Scheme FRGS/1/2016/STG08/UTP/01/1, e-Science fund grant scheme 06-01-02-SF 1140, and GUP-2016-024. The authors would also like to acknowledge the support of the staff and facilities at Geology Program and Faculty of Science and Technology, Universiti Kebangsaan Malaysia.

## REFERENCES

Abdul Ghani Rafek and Goh, T.L., 2012. Correlation of joint roughness coefficient (JRC) and peak friction angles of discontinuities of Malaysian Schists. *Earth Science Research*; 1(1):57-63

Abdul Ghani Rafek, Goh T. L., Askury A. Kadir, Chow, W. S., Choong, C. M., & Norbert, S. 2015. Application of slope mass rating for quantification of rock slope stability: case studies of Kinta Limestone, Ipoh, Perak. *Proceeding of International Conference on Slopes, Malaysia 2015* : 79-85.

Chow, W. S., & Majid Sahat. 1988. *Batu Runtuh di Gunung Tunggul, Gopeng, Perak*. Geological Survey Report. Ipoh: Minerals & Geoscience Department, Malaysia, 1/1988.

Foo, K. Y., (1983); *The Paleozoic Sedimentary Rocks of Peninsular Malaysia-Stratigraphy and Correlation*. *Proceeding of the Workshop on Stratigraphic Correlation of Thailand and Malaysia*; 1: 1-19.

Ghani Rafek, A., Goh, T.L., Hariri Arifin, M. 2012. Korelasi pekali kekasaran kekar dengan sudut geseran puncak satah ketakselajaran batuan Syis, Semenanjung Malaysia. *Sains Malaysiana* 41(3):293-297.

Ghani, R.A., Goh, T.L., Hariri, A.M. and Baizura, Y.N. 2011. Field and Laboratory-based Approach for the Determination of Friction Angle of Geological Discontinuities of Malaysian Granites. *Asean J. Sc. Technol. Dev.* 28(2):151-155.

Goh, T.L., Abdul Ghani, R., & Hariri, A. 2012b. Geomechanical Strength of Granites and Schists of Peninsular Malaysia. *Sains Malaysiana* 41(2):193-198.

Goh, T.L., Ghani Rafek, A. & Hariri Arifin, M. 2014a. Correlation of joint roughness coefficient with peak friction angles of discontinuity planes of granite, Peninsular Malaysia. *Sains Malaysiana* 43(5):751-756.

Goh, T.L., Abdul Ghani, R., Ailie, S.S., Norbert, S. and Lee K.E. 2014b. Empirical Correlation of Uniaxial Compressive Strength and Primary Wave Velocity of Malaysian Granites. *Electronic Journal Geotechnical Engineering* 19 (E) : 1063-1072.

Goh, T.L., Abdul Ghani, R., Ailie, S.S., Norbert, S., Lee K.E., and Azimah, H. 2015a. Empirical Correlation of Uniaxial Compressive Strength and Primary Wave Velocity of Malaysian Schists. *Electronic Journal Geotechnical Engineering* 20: 1801-1812.

Goh, T.L., Abdul Ghani, R., Ailie, S.S., Norbert, S., Azimah, H. and Lee K.E. 2015b. Correlation of Ultrasonic Velocity slowness with Uniaxial Compressive Strength of Schists in Malaysian. *Electronic Journal Geotechnical Engineering* 20: 12663-12670.

Goh, T.L., Abdul Ghani, R., Ailie, S.S., Azimah, H. and Lee K.E. 2016. Use of

Ultrasonic Velocity Travel Time to Estimate Uniaxial Compressive Strength of Granite and Schist in Malaysia. *Sains Malaysiana* 45(2):185-193.

Hoek, E. and Bray, J. (1981) *Rock Slope Engineering*, 3rd edn, Inst. Mining and Metallurgy, London, UK.

Hutchison, C. S., & Tan, N. K. (2009). *Geology of Peninsular Malaysia*. Kuala Lumpur: Geological Society of Malaysia.

ISRM (1978). Commission on standardization of laboratory and field tests. Suggested methods for the quantitative description of discontinuities in rock masses. *Int. J. Rock Mech. min. Sci.*, 15, No.6, 319-368. Reprinted in *Rock characterization and monitoring - ISRM suggested methods*, E. T. Brown (eds.), 1981, 3-52, Oxford: Pergamon .

Lai, K. H. (1974). *Rockfall Danger at the Southern End of Gunung Lang, Ipoh*. Geological Survey Report. Ipoh: Minerals & Geoscience Department, Malaysia.

Leman, M. S. (2013). Proposed Kinta Valley Geopark-utilizing Geological Resources for Environmental Quality Improvement and Society Well Being Enhancement. Keynote address. *Proceeding of the National Geoscience Conference*. Kinta Riverfront Hotel and Suites, Ipoh, Malaysia.

Norbert, S., Michael, C., Mairead, d. Abdul Ghani, R. and Rodeano, R. 2015a. Time series assessment on landslide occurrences in an area undergoing development. *Singapore Journal of Tropical Geography* 36 : 98-111.

Norbert, S., Muhammad Fahmi, A.G., Goh, T.L, Abdul Ghani, R., Azimah, H., Rodeano, R. and Lee, K.E. 2015b. Assessment of rockfall potential of limestone hills in the Kinta Valley. *Journal of Sustainability Science and Management* 10(2) 24-34

Norbert, S., Rodeano, R., Abdul Ghani, R., Goh, T.L., Noran, N.N.A., Kamilia, S., Nightingale, L.M., Azimah, H. and Lee, K.E. 2016. Rock Mass Assessment using Geological Strength Index (GSI) along the Ranau-Tambunan Road, Sabah, Malaysia. *Research Journal of Applied Sciences, Engineering and Technology* 12(1): 108-115

Norbert, S., Rodeano, R., Nightingale, L.M., Juhari, M. A., Abdul Ghani, R., Goh, T.L. 2014. Lineaments And Their Association With Landslide Occurrences Along The Ranau-Tambunan Road, Sabah. *Electronic Journal Geotechnical Engineering* 19 (c) : 645-656.

Priest, S. D. & Hudson, J.A. 1976. Discontinuity spacing in rock. *Int. J. Rock Mech. Min. Sci. And Geomech. Abst.*, 13 : 135-148

Ruhr University Bochum. 2016. Steereo 32. [<http://www.ruhr-uni-bochum.de/hardrock/downloads.html>]

Shu, Y. K., Lai, K. H. (1973). *Rockfall Danger at Gunung Lang Rifle Range Road, Ipoh*. Geological Survey Report. Ipoh: Minerals & Geoscience Department, Malaysia.

Shu, Y. K., Lai, K. H. (1974). *Rockfall at Gunung Cheroh, Ipoh*. Geological Survey Report. Ipoh: Minerals & Geoscience Department, Malaysia.

Shu, Y. K., Razak Y. A. (1984). *Rockfall at Gunung Pondok Padang Rengas, Perak*. Geological Survey Report. Ipoh: Minerals & Geoscience Department, Malaysia.